



*Supplement of*

## **Impacts of secondary ice production on Arctic mixed-phase clouds based on ARM observations and CAM6 single-column model simulations**

**Xi Zhao et al.**

*Correspondence to:* Xiaohong Liu ([xiaohong.liu@tamu.edu](mailto:xiaohong.liu@tamu.edu))

The copyright of individual parts of the supplement might differ from the article licence.

The conservations of mass and number mixing ratios are ensured in the modified scheme.

The tendencies of cloud hydrometeors are updated after we consider the SIP processes in the model. In the following equations, SIP related terms are in italic font and other processes are in the standard font:

For cloud ice:

$$\begin{aligned} \text{nitend} &= \text{nnuccd} + \text{nnucct} + \text{nnuccc} + \text{nnudep} + \text{nsacwi} + \text{nsubi} - \text{nprci} - \text{nprai} + \text{nnuccri} + \\ &\text{nf\_1mode} + \text{nf\_2mode} + \text{nf\_isc} + \text{nf\_ssc} + \text{nf\_gisc} + \text{nf\_ggc} \\ \text{qitend} &= \text{mnuccc} + \text{mnucct} + \text{mnudep} + \text{msacwi} - \text{prci} - \text{prai} + \text{vap\_dep} + \text{berg} + \\ &\text{ice\_sublim} + \text{mnuccd} + \text{mnuccri} + \text{mf\_1mode} + \text{mf\_2mode} + \text{mf\_isc} + \text{mf\_ssc} + \text{mf\_gisc} \\ &+ \text{mf\_ggc} \end{aligned}$$

For rain:

$$\begin{aligned} \text{nrtend} &= \text{nprc} + (\text{nsubr} - \text{npracs} - \text{nnuccr} - \text{nnuccri} + \text{nragg} - \text{nsipr}) \\ \text{qrtend} &= \text{pra} + \text{prc} + \text{pre} - \text{pracs} - \text{mnuccr} - \text{mnuccri} - (\text{mf\_1mode} + \text{mf\_2mode} + \\ &\text{mf\_big}) \end{aligned}$$

For snow:

$$\begin{aligned} \text{nstend} &= \text{nsubs} + \text{nsagg} + \text{nnuccr} + \text{nprci} + \text{nf\_big} - \text{nsips} \\ \text{qstend} &= \text{prai} + \text{prci} + \text{psacws} + \text{bergs} + \text{prds} + \text{pracs} + \text{mnuccr} + \text{mf\_big} - \text{mf\_isc} - \\ &\text{mf\_ssc} - \text{mf\_gisc} - \text{mf\_ggc} \end{aligned}$$

in which the process names are listed as follows:

nnuccd/mnuccd	homogeneous and heterogeneous nucleation from water vapor
nnucct/mnucct	contact freezing of cloud water
nnuccc/mnuccc	immersion freezing of cloud water
nnudep/mnudep	deposition nucleation in mixed-phase clouds
nsacwi/msacwi	H-M splintering
nprci/prci	autoconversion of cloud ice to snow
nprai/prai	accretion of cloud ice by snow
nnuccri/mnuccri	freezing of rain to form ice
vap_dep	deposition of cloud ice
ice_sublim/nsubi	sublimation of cloud ice
berg	WBF between cloud water and cloud ice
nprc/prc	autoconversion of cloud droplet to rain
nsubr/pre	evaporation of rain
npracs/pracs	collection of rain by snow
nnuccr/mnuccr	freezing of rain to form snow
nragg	self-collection of rain
pra	accretion of cloud water by rain
nsubs	sublimation of snow
nsagg	self-aggregation of snow
psacws	collection of droplets by snow
bergs	WBF between cloud water and snow
prds	sublimation of snow
nf_1mode/mf_1mode	SIP from the first mode of freezing rain break-up
nf_big/mf_big	SIP from the first mode of freezing rain break-up (big fragments)
nf_2mode/mf_2mode	SIP from the second mode of freezing rain break-up
nf_isc/mf_isc	SIP from cloud ice and snow collision
nf_ssc/mf_ssc	SIP from snow and snow collision
nf_gisc/mf_gisc	SIP from graupel and cloud ice/snow collision
nf_ggc/mf_ggc	SIP from graupel and graupel collision
nsipr	decrease of rain number due to SIP
nsips	decrease of snow number due to SIP

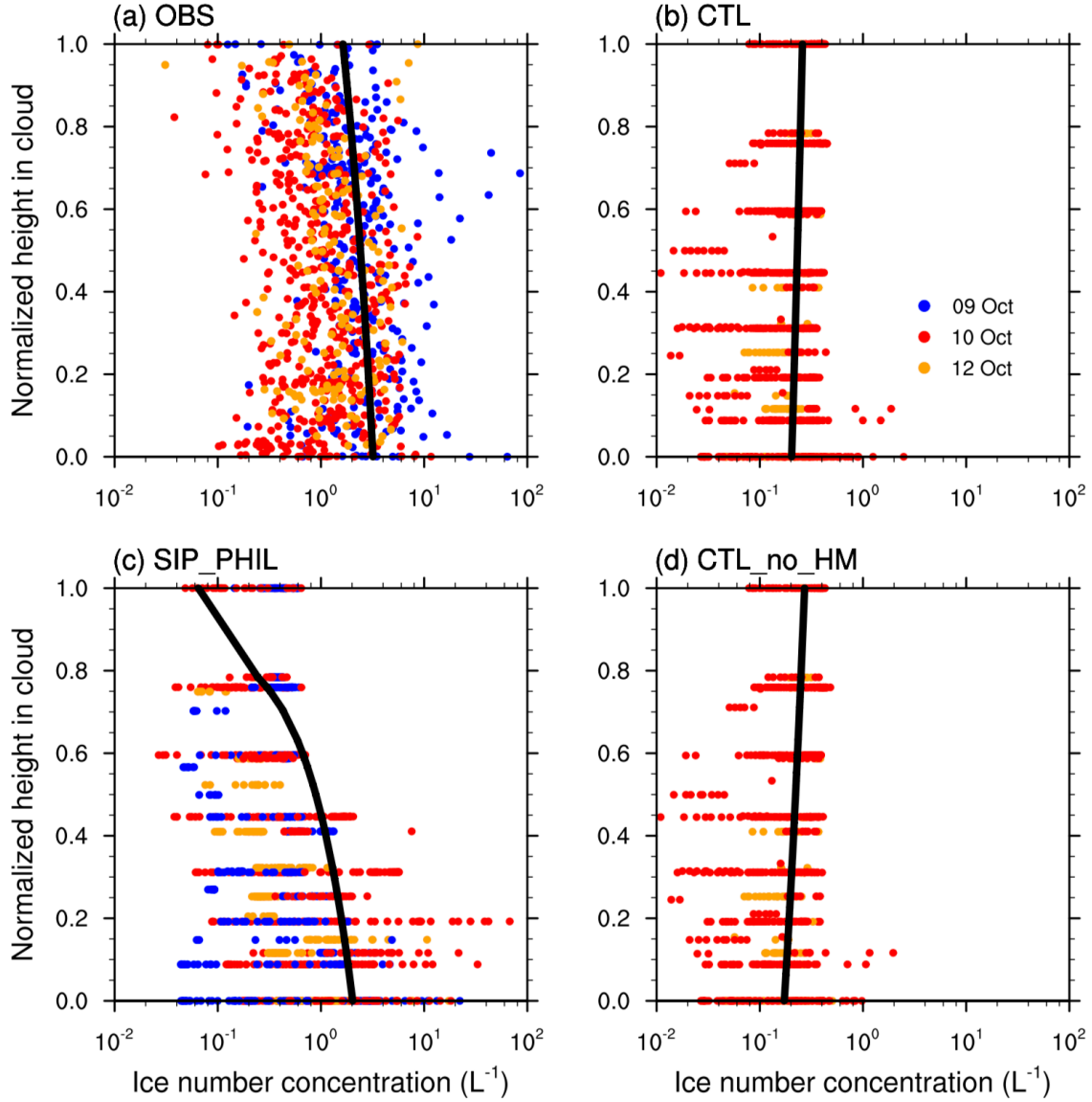


Figure S1. Ice number concentrations as a function of normalized cloud height from cloud base from (a) observation, (b) CTL, (c) SIP\_PHIL, and (d) CTL\_no\_HM. Black solid lines show the linear regression between ice number concentration and height. Only ice particles with diameters larger than 53  $\mu\text{m}$  from observations and model simulations are included in the comparison, no anti-shattering tip is adopted in this Figure.

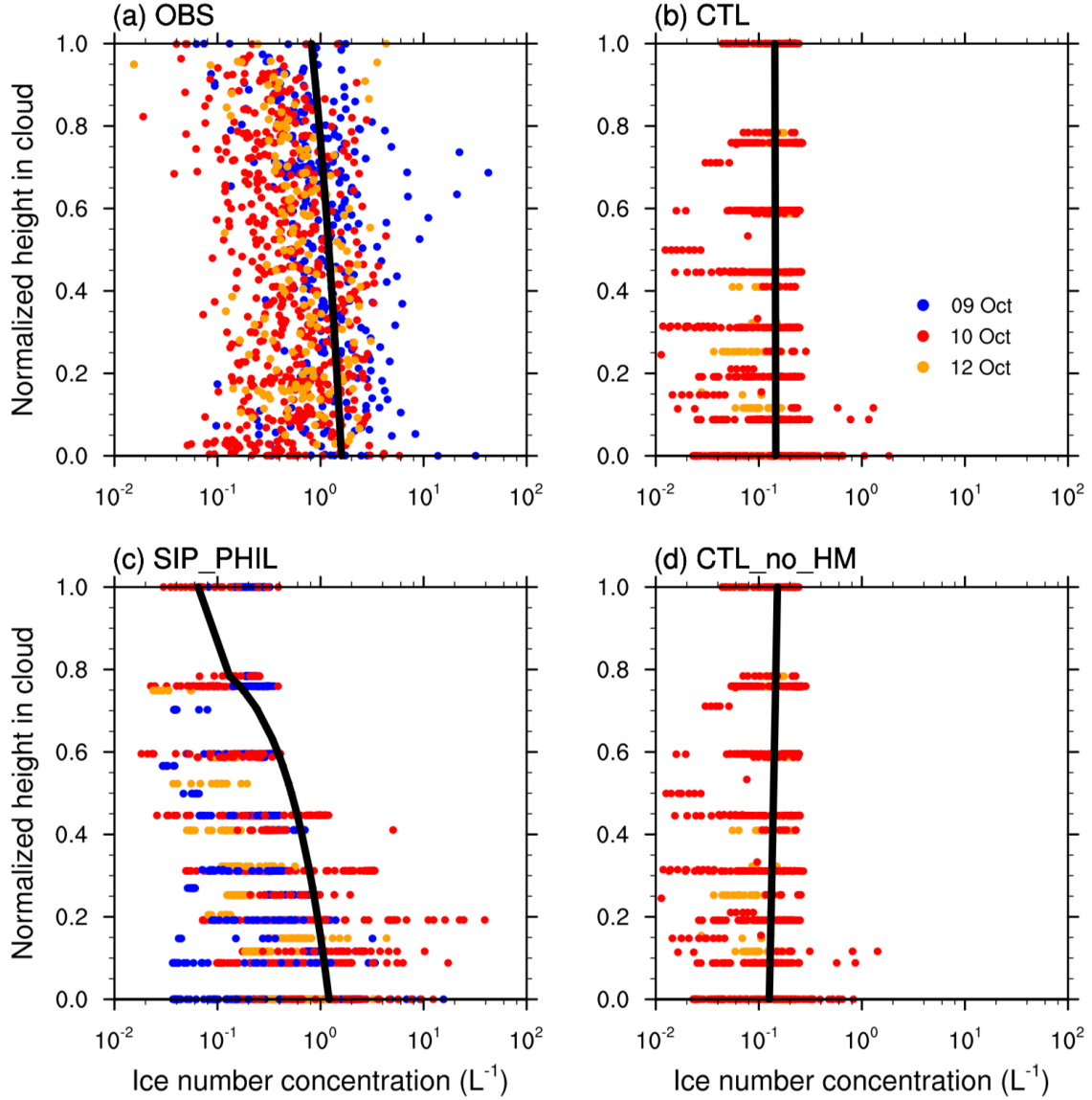


Figure S2. Ice number concentrations as a function of normalized cloud height from cloud base from (a) observation, (b) CTL, (c) SIP\_PHIL, and (d) CTL\_no\_HM. Black solid lines show the linear regression between ice number concentration and height. Only ice particles with diameters larger than  $100 \mu m$  from observations and model simulations are included in the comparison. A correction factor of  $1/2$  is applied to the observed ice number concentrations in (a).

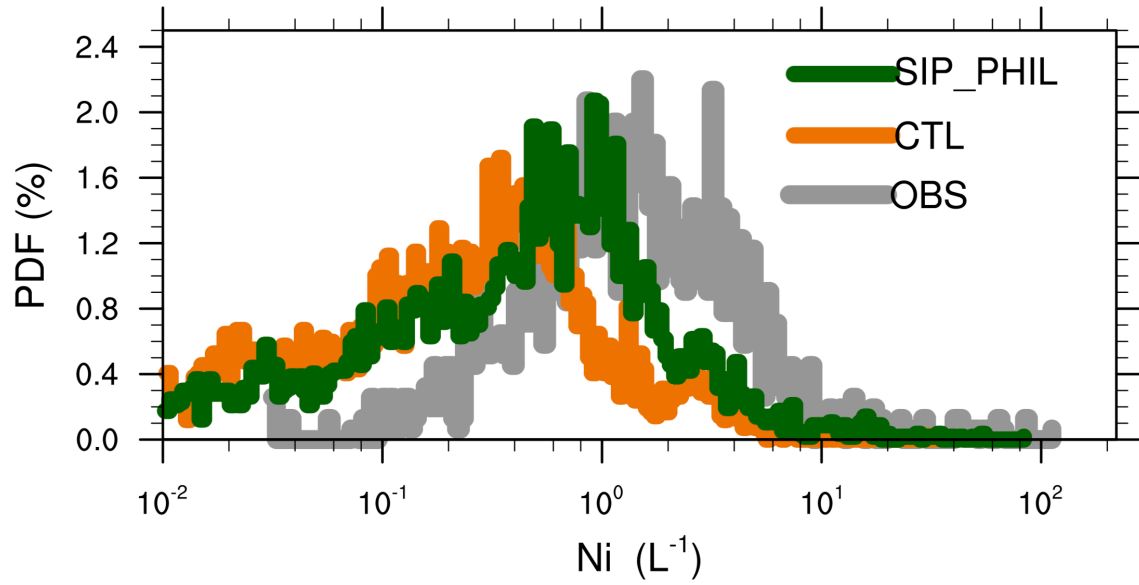


Figure S3. The probability density function (PDF) of ice crystal number concentrations from observation (gray line), CTL (orange line), and SIP\_PHIL simulations (green line). Only ice particles with diameters larger than  $53 \mu m$  from observations and model simulations are included in the comparison, no anti-shattering tip is adopted in this Figure.

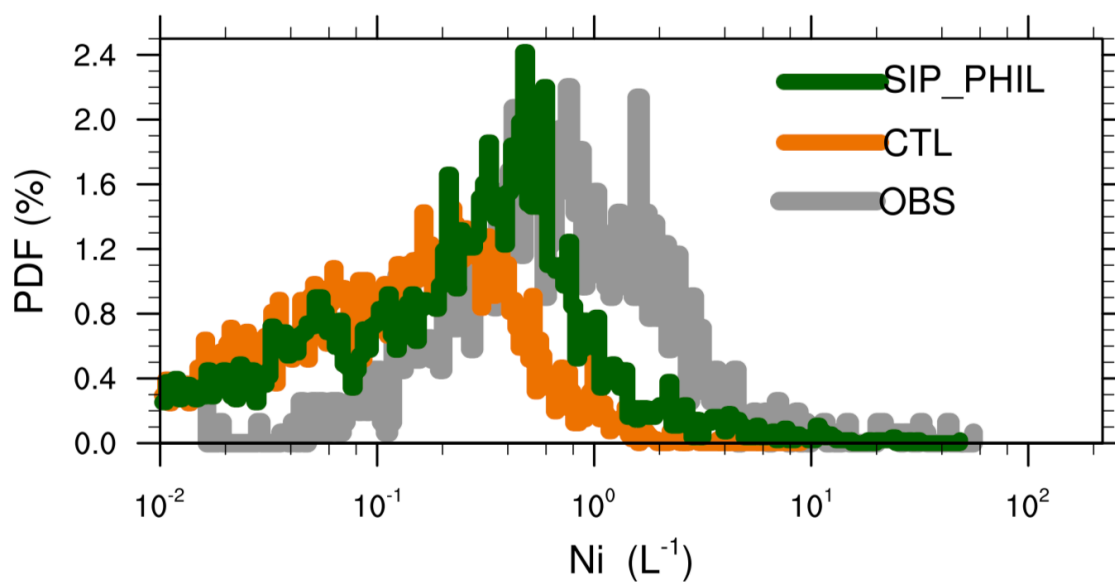


Figure S4. The probability density function (PDF) of ice crystal number concentrations from observation (gray line), CTL (orange line), and SIP\_PHIL simulations (green line). Only ice particles with diameters larger than  $100 \mu m$  from observations and model simulations are included in the comparison. A correction factor of  $1/2$  is applied to the observed ice number concentrations.

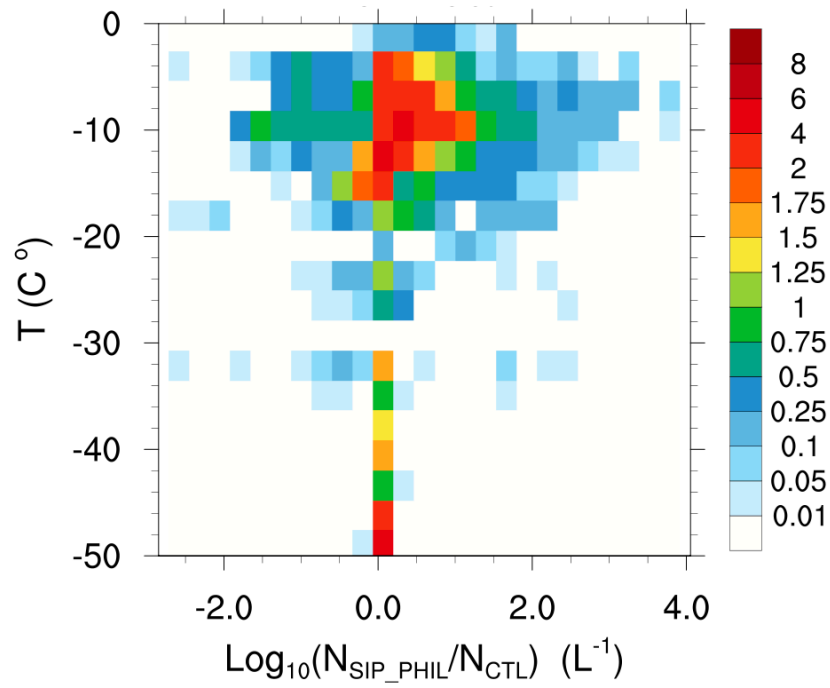


Figure S5. Bivariate joint probability density function of ice enhancement defined in terms of both temperature and ice enhancement. The ice enhancement is defined as  $\text{Log}_{10}(\text{N}_{\text{SIP\_PHIL}} / \text{N}_{\text{CTL}})$ .